*Revised Manuscript with No Changes Marked

Life-cycle assessment of a low-concentration PV module for building south wall integration in China

Guiqiang Li[1]*, Qingdong Xuan[1], Gang Pei[1]*, Yuehong Su[2], Yashun Lu[1], Jie Ji[1]

[1] *Department of Thermal Science and Energy Engineering, University of Science and Technology of China, 96 Jinzhai Road, Hefei City 230026, China*

[2]*Institute of Sustainable Energy Technology, University of Nottingham, University Park, Nottingham NG7 2RD, UK*

*Corresponding authors. Tel/Fax: +86 551 63603512. E-mail: ligq@mail.ustc.edu.cn; peigang@ustc.edu.cn;

Abstract: Low-concentration PV (CPV, concentrating photovoltaic) technology is a promising concept because it can work with the fixed installation. However, besides the economic consideration, the environmental impacts of the CPV module throughout its life cycle should be addressed as compared with the flat PV technology. Thus, in this paper, a novel high optical performance low-concentration concentrator namely asymmetric compound parabolic concentrator (aCPC) for building south wall integration is proposed. And based on the proposed aCPC-PV module, a life cycle assessment (LCA) has been performed for the low-concentration PV in China to make a scientific comparison with the PV module with the same output level environmentally. Several environmental indicators are calculated for Beijing, Hefei, Lhasa, Lanzhou, Harbin. The primary energy demand, energy payback time and environmental impacts are considered over the entire life cycle of the aCPC-PV module. The results show that the primary energy demand, energy payback time and environmental impacts of the aCPC-PV module are all relatively lower than that of the PV module with the same output. It is confirmed by the LCA study that the aCPC-PV module on behalf of the low-concentration PV technology is still a feasible and effective way for actual engineering because it's more economic and more environmental friendly than the PV technology although the PV is experiencing continuous decrease in price and increase in efficiency.

Keywords: asymmetric compound parabolic concentrator (aCPC); optical efficiency; life-cycle assessment (LCA); energy payback time (EPBT); environmental impacts.

1 Introduction

Energy is vital for the development of every country which is related to every aspect of the regular and efficient operation for human activities such as the transportation, industry, agriculture and human daily life, etc. However, present energy structure still mostly depends on the non-renewable energy resource, for example, coal, petroleum, and natural gas. It has been stated that the vast majority of greenhouse gases come from the energy production or consumption, and almost 70% of the worldwide energy demand is provided by fossil fuels. Besides, electricity generation is responsible for 40% of global CO_2 emissions [1]. The drawbacks of the vast consumption of fossil energy are obvious, and can be concluded as: on the one hand, the non-renewable energy will finally be exhausted as its availability is in decreasing trend now [2]; on the other hand, the combustion of the fossil energy releases a large amount of greenhouse gas and toxic emissions, such as sulfide, nitric oxide (NOx), phosphate, etc.[3] which will cause many environmental problems, for example, greenhouse effect, haze and river pollution, etc.[4]. Air/water/soil pollution and greenhouse gas emissions are becoming major concerns in some developing countries [5] especially for China, one of the largest developing countries. The data in 2014 revealed that coal accounts for more than 66% of China's primary energy demand. Due to its rapid development causing higher energy consumption than any other country, energy structure transformation and upgrading is urgent for China.

As the energy security and climate change problems have become more and more serious, solar power utilization has received increased attention throughout the word [7, 8]. In this area, solar-to-electricity conversion (Photovoltaic technology) as a clean energy resource which converts solar energy directly into the electricity has experienced a sharp growth during the last decades [9, 10]. China has now become one of the largest manufacturer and consumer of PV products in the world [11] which makes a significant impact on the world's renewable energy development and solar PV industrial sector [12]. Although PV technology is clean and renewable, it will also cause environmental issues [13] due to the energy and material consumption during the processes of production, transportation, installation, maintenance and dismantling. The recovery and disposal of the PV system, especially the process of solar grade silicon will consume a large amount of electricity.

Speaking of the PV application, low-concentration PV technology is an interesting topic because it can work as a static concentrator for it doesn't need the tracking system or seasonal adjustment. Besides this, it can also reduce the amount of PV cells used by using low cost PMMA material to produce the same or even higher DC output [14, 15] and harvest a higher temperature energy resource as well, which will be beneficial for the building integrated concentrating photovoltaic/thermal systems (BICPV/T). The concentrators are usually designed in reflective and/or refractive forms to concentrate the solar radiation onto the receiver where the PV cell is attached [16].

A new report from research and consulting firm Global Data stated that the global Concentrated Photovoltaic (CPV) market is expected to undergo a major growth spurt in the next several years, with its cumulative installed capacity forecasted to jump from 357.9 Megawatts (MW) in 2014 to 1043.96 MW by 2020 [17]. As for the BICPV, there is no doubt that it will attract more and more attention in future. There are several different low-concentration PV systems that have been studied in the last years, and they will be presented in detail in the next section to show the benefits of low-concentration PV technology.

Abu-Bakar et al. proposed a novel rotationally asymmetrical compound parabolic concentrator (RCPC) for application in BICPV systems [18]. The simulation work was conducted by using the software ZEMAX® and a maximum optical concentration gain as high as 6.18X when compared with the non-concentrating cell was observed. Furthermore, experimental work using a solar simulator for a RACPC-PV with a concentration ratio of 3.667X was conducted, and it was found that the RACPC increased the short circuit current and the maximum power by 3.01X and 3.33X respectively compared with a bare cell [19]. Mallick et al. designed a novel asymmetric CPC which consists of two different parabolas in the formation of the reflection, and then he further proposed a second generation PRIDE (Photovoltaic Facades of Reduced Costs Incorporating Devices with Optically Concentrating Elements) concentrator [20], and the experimental results at Northern Ireland (54°36'N, 5°37'W) confirmed that the asymmetric CPC is a feasible technology that can be used on the building façade. Su et al. proposed a novel symmetric lens-walled structure for CPC namely lens-walled CPC for PV applications [21], and Li et al. elaborated on the structure optimization of the lens-walled CPC [22] and analyzed its flux distribution compared with the mirror CPC [23]. The advantages of the lens-walled CPC can be concluded as; more uniform flux distribution and larger acceptance angle than those of the mirror CPC and 80% optical performance of the dielectric CPC but less dielectric material with the same geometrical concentration ratio. In order to increase the optical efficiency of the lens-walled CPC, Li et al. further proposed a novel lens-walled CPC with air gap between the lens structure and the mirror, thus it can adopt both the total internal reflection and the specular reflection to collect sun rays [24]. The simulation and experimental results showed that the optimization structure by adopting the total internal reflection can increase the optical efficiency by more than 10%. Then they built a CPV/T system based on the optimized lens-walled CPC for application on buildings [25-27], numerical and experimental results showed a good concentrating PV/T performance which proved a solution for BICPV or BICPV/T.

It has been proved that the lens-structure for the CPC has many advantages, such as: larger acceptance angle; more uniform flux distribution; less dielectric material. Based on the lens-walled structure, a novel asymmetric lens-walled CPC (aCPC) which is composed of the asymmetric compound parabolic curves for integration with building south wall is proposed. The prototype of the aCPC-PV module is manufactured and fabricated, and it has been analyzed in detail based on the simulation and the experiment results. The experimental results reveal that the average experimental optical efficiency is 74% and the ratio of the maximum power obtained from the aCPC-PV to that obtained from the non-concentrating PV is 1.74X. It is proved by both the experiment and the simulation work that the aCPC has a large acceptance angle of 60° with high optical efficiency. In this case, the aCPC will be a good choice for the application of BICPV or BICPV/T systems on the building south wall. In addition, considering that at different latitude areas, the incidence angles of the sun rays may vary a lot. In order to make the aCPC more suitable for different areas, the optimization structure is also proposed, and the optimized aCPC has similar optical performance with the original aCPC.

However, due to the continuous decrease in the cost of PV cells and the increase in their efficiency [28], the cost advantage of the low-concentration PV or PV/T systems for BI application seems to be weaken. But the call for zero net anthropogenic greenhouse gas emissions is a common agreement among the countries in the world. So besides the economic aspect, the environmental impacts and energy payback time should be taken into consideration. The aCPC model is an interesting topic which also shows a good potential for covering the energy demand for the buildings, especially for China. Therefore, studies about the aCPC-PV module's environmental profile, by means of life cycle assessment (LCA) would be useful for policy making by providing analytical evaluation environmentally [29]. In this way, the LCA study of the aCPC-PV will further provide a scientific comparison between the non-concentrating PV and low-concentration PV, showing that BICPV or BICPVT is still both more economic and more environmental friendly as compared with the non-concentrating PV.

LCA is a globally accepted tool to identify the environmental impacts involved in every process from cradle to grave systematically for a product, which can be used in wider fields including the PV and CPV systems [30, 31]. Several researchers have performed LCA studies for the PV systems. Sagani et al. presented an LCA analysis of relatively small rooftop PV-grid-interconnected energy systems of 2–10 kWp rated power, located in Athens, Greece [32]. Yu et al. performed an LCA study for grid-connected electricity generation from a metallurgical route multi-crystalline silicon (multi-Si) photovoltaic (PV) system in China [33]. Kim et al. analyzed the environmental loads of 100 kWp cadmium telluride photovoltaic (CdTe PV) power generation systems in Malaysia by using LCA method [34]. Hong et al. conducted a study to identify the environmental impacts throughout the production process of multi-crystalline silicon (multi-Si) in China by life cycle assessment [35]. Jayathissa et al. assessed the environmental impacts of a dynamic, adaptive, building integrated photovoltaic (BIPV) systems which combine the benefits of adaptive shading with facade integrated solar tracking [36]. Kabakian et al. compared the impact of the current Lebanese electricity system with production of electricity from PV and highlighted that PV systems are environmentally better than centralized electricity systems [37]. Lu et al. analyzed the environmental payback time of the roof-mounted building-integrated photovoltaic (BIPV) system (grid-connected) in Hong Kong and the EPBT (energy payback time) and GPBT (greenhouse-gas payback time) of the PV system were estimated to be 7.3 years and 5.2 years respectively [38]. Hou et al. also conducted the life cycle assessment of grid-connected photovoltaic power generation from crystalline silicon solar modules in China aimed at providing useful information to enact reasonable policies, development targets, as well as subsidies for PV technology in China [39].

As for the low-concentration PV systems for BI application, a number of studies have also been done by researchers. Lamnatou et al. conducted a life cycle assessment of a linear dielectric-based concentrating photovoltaic for building integrated applications for Exeter, Barcelona, Madrid, Dublin and Paris based on Embodied Energy (EE) and Embodied Carbon (EC) [40]. Furthermore, Lamnatou et al. performed an advancement study towards the life cycle assessment (LCA) of a linear dielectric-based building-integrated concentrating PV system by means of multiple life-cycle impact assessment methods and environmental indicators such as: ReCiPe, Eco-indicator 99, ecological footprint, USEtox, ReCiPe-based and Eco-indicator-99-based payback times (PBTs), etc. [41]. Then based on the dielectric-based 3D building-integrated concentrating photovoltaic modules, Lamnatou et al. [42] did the same LCA study as the Ref. [41] for different scenarios: Barcelona, Seville, Paris, Marseille, London and Aberdeen. Menouf et al. conducted an LCA study of a Building Integrated Concentrated Photovoltaic (BICPV) scheme which is composed of 22 flat coated reflectors at the University of Lleida (Spain) [43]. Within the area of the large-scale, high-concentration PV systems, Fthenakis and Kim investigated the EPBT, GHG emissions, land transformation, etc. [44] for the Amonix 7700 HCPV system during its life cycle and the results revealed that although operating high-concentration PV systems require considerable maintenance, their life cycle environmental burden is much lower than that of the flat-plate c-Si systems operating in the same high-insolation regions. Peharz and Dimroth evaluated the energy payback time of the high-concentration photovoltaic system FLATCON® using III–V semi-conductor multi-junction solar cells [45]. Nishimura et al. evaluated the environmental impacts and EPBT of a high-concentration photovoltaic power generation system by hypothetical case studies in Toyohashi, Japan and Gobi desert in China and the results showed that Gobi desert is the most appropriate location of the high-concentration photovoltaic power generation system with the consideration of the EPBT [46].

From the literature review, the following can be concluded: low-concentration PV technology is a promising concept because it can work as a static concentrator without any tracking systems or seasonal adjustments and this shows benefits of the CPV or CPV/T systems for building application; It can also reduce the amount of PV cells used by using the low cost PMMA material to produce the same or even higher DC output and harvest a higher temperature energy resource as well; China is the country with a large population, as the society develops, the energy demands of the buildings will experience a rapid growth in the next decades, and the low-concentration PV technology would be a good solution to such problem.

However due to the continuous decrease in the cost of the PV cells and increase in their efficiency, the cost and performance advantages of the large-scale application of the low-concentration PV technology seem to be weaken. For this reason, it’s vital to conduct the life cycle assessment for it as compared with the non-concentrating PV technology to show the advantages of the low-concentration PV technology clearly and scientifically thus to encourage its development all over the world. In addition, it’s clear from the above presentation that within the area of the PV applications on the buildings in China, the LCA study are mainly about non-concentrating PV systems, while in other countries such as Europe and America countries, the LCA studies for non-concentrating PV, low-concentration PV and large scale/high concentration ratio CPV systems have all been involved. To date, to the best of the authors’ knowledge, there has been no LCA studies that were conducted for the low-concentration CPV systems in China and there are fewer studies about its environmental comparison with the non-concentrating PV technology in the world. This further highlights the necessity to conduct the life cycle assessment for the proposed aCPC-PV module and quantify its environmental impacts in China thus to provide a scientific basic for policy-making of the local government in terms of developing the Chinese building-south-wall-integration concentrating PV industry. In addition, the LCA study of the aCPC-PV will provide the general method and basic data for the environmental evaluation of other kinds of low-concentration CPV systems for application in China. On the one hand, the paper aims to fill in gaps of LCA studies of low-concentration PV technology in China since it's urgent for China to find a good solution to the vast building energy demand and low-concentration PV technology is a good way. Furthermore, the LCA study of the low-concentration PV technology highlights its comparison with the non-concentrating PV technology to show its advantages environmentally and scientifically.

In this study, the environmental impacts for the aCPC-PV module for application in China is evaluated in detail. The LCIA method CML2001- Apr. 2013. is used to process the analysis. Considering that the lifespan time of the PV system is usually longer than 25 years [47], and the time to recycle the PV in China is far from the deadline, so the disposal stage is not considered in the study. In addition, the energy demand during the usage stage is also not taking into consideration because the data is unavailable and the consumption is less in this stage which has little impact on the environment [48].

2. The description of the aCPC-PV module/material, methods and the scope of the study

2.1 Geometric and optical characteristics of the aCPC

The geometric structure of the aCPC is shown in Fig.1, the profile curve $P'M'N'Q'NMP'$ is the inner part of the original aCPC: the outer contour of the lens consists of two asymmetric compound parabola curves MP and NQ . Detailed information about how the lens structure is formed can be found in [23] and the equations of the compound parabola curves can be gotten from [23] or [49]. The distance between MN and $M'N'$ is the base height. The geometrical concentration ratio of the aCPC is 2.57X, according to Eq. (1).

$$C = \frac{P'Q'}{MN} \quad (1)$$

In order to collect the escaped sun rays to improve the optical performance of the aCPC, an asymmetric mirror CPC is also integrated with the asymmetric lens-walled structure. In this way, the escape sun rays can be collected by the specular reflection.

The angle between the normal of the base of the aCPC and the incident ray is defined as the incidence angle of the sun ray for the aCPC. For the original aCPC, the incidence angle is θ' while for the optimization aCPC, the incidence angle will be θ.

It should be noted that incidence angles of sun rays at different latitude areas may vary a lot. In order to make the aCPC more suitable for different locations, the structure of the aCPC is further optimized. The optimization structure is formed by rotating the original aCPC around the up end point M away from the wall ML by a certain angle β. Then the profile curve becomes $MLNQ'N'M'P'M$. It still has many advantages such as easy arrangement, sufficient utilization, etc. to attach the absorber of the aCPC to the building south wall. So the mirror NL is added to achieve this goal. It's obvious that the incidence angle for the optimization aCPC will be θ ($\theta = \theta' - \beta$), which indicates that the acceptance range from 0°—60° extends to β—(β +60°). For example, if the rotation angle is 15°, the acceptance range will be 15°—75°.

The configuration of the aCPC-PV module is depicted in Fig. 2. The PV cell is attached with the absorber of the aCPC, and for the application on the buildings, the front glass cover is adopted to prevent the dust and rain drops falling on the inner surface of the concentrator to reduce the overheads during the lifecycle. In order to find out the electrical characteristics of the aCPC-PV, the module of the aCPC integrated with a PV cell (Fig.3) is manufactured and fabricated. The experiment for the aCPC-PV module is conducted by a solar simulator (Oriel® Solar Simulator 94043A, Newport Stratford Inc.®, USA) (ray intensity is 1000 W m^{-2}, uniform illumination is less than 2% in an active area of 100X100 mm^2). The experiment setup is shown in Fig.3. The actual optical efficiency (gotten from the experiment) and the simulation optical efficiency (performed by the Lighttools®, a fast and accurate ray tracing software) are presented in Fig. 4. From the results, it can be seen clearly that the experiment results and simulation results showed a good agreement. The average experiment optical efficiency is 74% and this value is 86.6% for the simulation results. Detailed fitted equations of the simulation and experimental optical efficiency of the aCPC can be expressed by:

$$\begin{aligned} y_1 = & -10^{-8} x^5 + 1.14\times10^{-6} x^4 - 5.54\times10^{-5} x^3 + \\ & 8.12\times10^{-4} x^2 + 8.06\times10^{-4} x + 0.87 \end{aligned} \tag{2}$$

$$\begin{aligned} y_2 = & -10^{-8} x^5 + 9.3\times10^{-7} x^4 - 5.42\times10^{-5} x^3 + \\ & 1.18\times10^{-3} x^2 - 5.04\times10^{-3} x + 0.67 \end{aligned} \tag{3}$$

Where Eq. (2) is the simulation optical efficiency; Eq. (3) is the experiment optical efficiency; y – the optical efficiency of the aCPC (η_{opt}); x – the incidence angle of the sun rays (θ), °.

In order to calculate the annual energy collection of the aCPC, the optical efficiency for the diffuse solar radiation collection should be determined as well. It has been stated that this value is almost constant for the diffuse solar radiation at different incidence angles [50, 51]. According to the simulation, the optical efficiency for the diffuse solar radiation collection is 50% for the aCPC.

2.2 System boundary, life cycle inventory and data sources

The goal of this study is to present the life cycle assessment of the proposed aCPC-PV module for integration with the building south wall and quantify its environmental impacts in China.

The functional unit of the studied module is 1 kWp electricity supply, and the system boundary is shown in Fig. 5. The aCPC module and PV cells are manufactured separately and then assembled together. For the aCPC, the system boundary contains the production process of the polymethyl methacrylate (PMMA), and the fabrication process of the aCPC which includes the lens and mirrors as well as the silver coating of the reflection mirrors. It is hypothesized that for the production of the aCPC model, once the Methl Methacrylate (MMA) is transformed into the PMMA through the polymerization reaction, the hot liquid PMMA is bumped into the metal model of the aCPC directly, then the prototype will be shaped up. This kind of method is called gravity die casting which is widely used for the production of the precise objects. And the advantages of this technology are cheap, exquisite and energy-saving compared with the CNC wire cutting. Using this technology will be beneficial for the vast production of the aCPC model. As for the production of the PV cells, the system boundary includes the upstream processes, which involves the silica extraction and crystalline silicon bar/ingot growth, and midstream processes (cell fabrication). Finally, the assembling of the aCPC-PV module is considered which includes the aluminum frame, front glass and other additional components production. It is assumed that the aCPC and the PV cells are produced at the same place with the hypothesis that the aCPC-PV module has been widely acknowledged and the industry for it has been developed thoroughly. In this case, the transportation (by truck) of the materials/components from the factory gate to the building is considered only, and an average distance of 150 km is assumed.

The inventory data, including the material consumption and environmental emissions involved in the production of the aCPC and PV cell are mainly from Chinese companies and some are also from GaBi® software and Ecoinvent v3.01 database based on the recommendations provided by the ISO 14040:2006 [52]/ISO 14044:2006 [53]. In Table 1, details about the materials for the aCPC-PV module (1kWp) and for the additional components (related to the BOS) are presented.

2.3 Life-cycle impact assessment (LCIA)

The goal of the life-cycle impact assessment (LCIA) is to identify and evaluate the amount and significance of the potential environmental impacts for a specific system throughout its life cycle. LCIA is composed of the mandatory elements which include the relevant impact categories' selection, classification and characterization (in this stage, the inputs and outputs are assigned to impact categories and their potential impacts are quantified according to characterization factors) and the optional elements, such as normalization, grouping and weighting.

Many LCIA methods have been developed since the LCA studies first appeared which can be accessed from the current database of LCA dedicated software on the market, such as GaBi®, SimaPro 8®, etc. These methods are continuously researched and developed by different scientific groups based on different methodologies. For LCIA methods, there are two main approaches for the classification and characterization of the environmental impacts: one is the problem-oriented approach (mid-point), the other one is the damage-oriented approach (end-point) [54]. In this study, CML2001- Apr. 2013 is used to make the life-cycle impact assessment for the aCPC-PV module. The so-called CML method is the methodology of the Centre for Environmental Studies of the University of Leiden, which focuses on a series of environmental impact categories expressed in terms of emissions to the environment. Detailed information about the CML method can be found at the Centre for Environmental Studies (CML), University of Leiden [55].

3. Primary energy demand and energy payback time (EPBT)

Based on the data source in China, the primary energy demand for the proposed aCPC-PV module from non-renewable and renewable resources is 12.2 MJ/Wp, and detailed results are shown in Fig. 6.

Energy payback time (EPBT) is widely used for the identification of the ratio of the input and output, and the equation that has been widely used for the PV systems is adopted, which is expressed as:

$$EPBT = \frac{E_{in}}{E_{agen}} = \frac{E_{mat} + E_{inst} + E_{transp}}{E_{agen}} \ (years) \quad (4)$$

Where E_{in} – the total energy input for the production of the aCPC-PV module, including the manufacturing of the materials, the PV cells, aCPC modules and the additional components, the installation and transportation of the system; E_{mat} – the primary energy demand for materials manufacturing; E_{trans} –the total energy needed for the transportation; E_{inst} – the primary energy demand related to the installation of the system; E_{agen} – the annual electricity generation;

For the calculation of the annual electricity generation, the following equation is adopted:

$$E_{agen} = \int_{t_1}^{t_2} \left(G_{dir} \cdot \eta_{opt} + G_{diff} \cdot \eta_{opt,diff} \right) \cdot A \cdot \eta_{efficiency} dt \quad (5)$$

Where G_{dir} – the total direct solar irradiance on the building south wall, Wm^{-2}; G_{diff} – the diffuse solar irradiance on the building south wall, Wm^{-2}; η_{opt} – the optical efficiency for the collection of the direct solar radiation; $\eta_{opt,diff}$ – the optical efficiency for the collection of the diffuse solar radiation (50%, from the software simulation); A – the area of the front aperture, m^2; $\eta_{efficiecny}$ – the electrical efficiency of the PV cell.

As for the calculation of the annual energy collection, the incidence angle of the sun ray at a specific time should be ascertained first (thus the optical efficiency at this time can be determined). In Fig. 7, detailed schematic of the incidence angle of the sun ray for the aCPC is depicted. It can be seen from Fig.7 clearly that the angle between the horizon and the projection of the direct solar radiation vector on the north–south vertical plane θ_{NS} (the N–S projected solar altitude angle) equals to θ, which could be further expressed by [27]:

$$\cos\theta_{NS} = \tan\alpha / \cos\gamma_s \tag{6}$$

Where α –solar altitude angle; γ_s – solar azimuth angle; θ – incidence angle for the aCPC.

It should be noted that the weather data of the typical year (which is gained from EnergyPlus) is usually the solar radiation on the horizontal surface. Thus in this study, the Hay and Davies, Klucher and Reindl models (HDKR) is used to calculate the solar radiation on the building south wall based on the data of that on the horizontal surface. It can be expressed by Eq. (6)-(13) [56].

For a surface with a declination angle of λ:

$$\begin{aligned} I_T = \left(I_b + I_d A_i\right) R_b + I_d (1 - \mathrm{A_i}) \left(\frac{1+\cos\lambda}{2}\right) \cdot \\ \left[1 + \mathrm{f}\sin^3\left(\frac{\lambda}{2}\right)\right] + I\rho\left(\frac{1-\cos\lambda}{2}\right) \end{aligned} \tag{7}$$

$$A_i = I_b / I_o \tag{8}$$

$$f = \sqrt{I_b / I} \tag{9}$$

$$R_b = \frac{I_{dir}}{I_b} = \frac{\cos\theta_T}{\cos\theta_Z} \tag{10}$$

$$\begin{aligned} \cos\theta_T = {} & \sin\delta\sin\varphi\cos\lambda - \sin\delta\cos\varphi\sin\lambda\cos\gamma + \\ & \cos\delta\cos\varphi\cos\lambda\cos\omega + \cos\delta\sin\lambda\sin\gamma\sin\omega + \\ & \cos\delta\sin\varphi\sin\lambda\cos\gamma\cos\omega \end{aligned} \tag{11}$$

$$\cos\theta z = \sin\alpha = \sin\varphi\sin\delta + \cos\varphi\cos\delta\cos\omega \quad (12)$$

$$\delta = 23.45\sin[360\times\frac{284+n}{365}] \quad (13)$$

Where I_b – direct solar radiation on the horizontal surface; I_d – diffuse solar radiation on the horizontal surface; A_i – Anisotropy index; R_b – View factor for beam radiation; λ – declination angle; I – total solar radiation on the horizontal surface; ρ – the reflectivity of the ground; θ_T – incidence angle of the solar rays on the decline surface; θ_Z – Zenith angle; δ – declination angle of the sun; φ – latitude angle; γ – azimuth angle of the declination surface; ω –Hour angle.

In this study, the azimuth angle of the south wall is assumed to be 0°, which means that the building south wall is due south. So the direct solar irradiation on the building south wall will be:

$$I_{southwall,\,dir} = I_b\frac{\cos\delta\sin\varphi\cos\omega - \sin\delta\cos\varphi}{\sin\delta\sin\varphi + \cos\varphi\cos\delta\cos\omega} \quad (14)$$

Where $I_{southwall,\,dir}$ –direct solar irradiance on the building south wall, Wm^{-2}.

In table 2, annual solar irradiance on the building south wall, annual electricity generation, total electricity generation for 20/30 years lifespan for Lhasa (91.11°E, 29.97°N), Hefei (117.27°E, 31.86°N), Lanzhou (103.73°E, 36.03°N), Beijing (116.46°E, 39.92°N), Harbin (126.63°E, 45.75°N) are presented.

Monthly electricity generation for five cities (Lhasa, Hefei, Lanzhou, Beijing, Harbin) where (a) is based on the experimental optical efficiency and (b) is based on the simulation optical efficiency is illustrated in Fig. 8. A performance degradation of 0.7% per year is considered for calculating the electricity production during 20/30 years lifespan [30]. From the results, it can be seen clearly that in summer months, the power output is lower than that of the other months. This can be explained by: In June to September, the solar altitude angle is very large. Although the solar intensity on the ground is very large, solar intensity on the building south wall is much lower. By comparison of Fig. 8 (a) and (b), it can be seen that the optical efficiency plays a vital role in the output of the aCPC-PV module, which suggests an effective way of improving the optical performance of the aCPC to increase the annual electricity generation of the system.

EPBTs of the aCPC-PV module (with the experimental/simulation optical efficiency) and PV systems (for 1kWp) for five different cities are shown in Fig. 9. From the results, it can be seen that Beijing has the lowest EPBT (2.82 years, experimental optical efficiency) while Hefei has the highest EPBT (4.74 years, experimental optical efficiency). This is related to the highest aCPC-PV output in Beijing and lowest in Hefei. While with the simulation optical efficiency, the EPBTs of five cities are around 0.5 years lower than that with the experimental optical efficiency. On the other hand, even with the experimental optical efficiency, EPBTs of the CPV system are always 0.2-0.3 yeas lower that of the PV system with the same total output.

4. Environmental results and interpretation

4.1 Acidification Potential (AP)

The air pollutants such as sulphur dioxide and nitrogen oxide will cause the acidification of soils and waters predominantly through the transformation of them into acids (H_2SO_4 and HNO_3). Due to the decrease in the pH-value of the rainwater as well as the fog, the ecosystem will be further damaged. The most prominent impact is the forest dieback. The AP is given in kg SO_2-equivalent/Wp.

The AP for the aCPC-PV modules is 9.16×10^{-3}kg SO_2-equivalent/Wp, and its values for different process flows are presented in Fig. 10. It should be noted that the major energy resource is from Chinese electricity grid which is mainly generated from the coal, and its combustion will release a large amount of nitrogen oxide. In the manufacturing processes of the PV cell and the aCPC model, the production of the solar-grade mono-Si and the transformation of the Methl Methacrylate (MMA) into the PMMA (through polymerization reaction) consume the bulk of the electricity input thus contribute most to the AP.

4.2 Global Warming Potential (GWP 100 years)

The mechanism of the greenhouse effect can be concluded as: a part of the incoming solar radiation will be absorbed by the earth's surface while the other part will be reflected as the infrared radiation. The reflected part is absorbed by the greenhouse gas in the troposphere and a portion of it will be re-radiated back to the earth. This is a simple thermodynamic problems, the heat gain is always lager than the heat loss which will finally increase the temperature of the earth. Global warming is a well-known environmental problem. The natural greenhouse effect is good for the earth to keep a relative warm environment, however human activity increases the amount of the greenhouse gas in the air which includes carbon dioxide, methane and CFCs. The global warming potential is given by carbon dioxide equivalents (CO_2-Eq.). Considering that residence time of the gases in the atmosphere is incorporated into the calculation, a period of 100 years is customary for the assessment.

The GWPs for the manufacturing of the PV cell, aCPC model and CPV systems are presented in Fig.11. From the results, the GWP for the aCPC-PV module is 1.092kg CO_2-Eq./Wp. It's clear that PV cells are the highest contributors to the GWP (accounts for around 50%). This is also related to the high electricity and steam consumption during the manufacturing process of the PV cells. It was mentioned in the last section that Chinese electricity is mainly from the coal which will release an amount of CO_2 during the combustion. The aCPC module contributes about 30% to the total GWP, this is proportional to the electricity consumption as well.

4.3 Eutrophication potential (EP)

Eutrophication is the enrichment of the nutrients such as nitrogen and phosphorus in the river or the lake, which will result in the rapid growth of the plants in the water. In turn, the duckweed on the water will prevent the sun lights from entering the inner depth of the water, which leads to a decrease in photosynthesis and less oxygen production. Finally, the fish and plants will die, and their dead body will experience anaerobic decomposition due to the lack of the oxygen. All of this would lead to the destruction of the ecosystem. It should be noted that nitrate and phosphate at low levels is good for the balance of the ecosystem and will do no harm to human, too. However, waste water from the factory contains abundant nitrate and phosphate, and its discharge into the river will cause the so-called eutrophication. The eutrophication potential is calculated in phosphate equivalents (PO_4-Eq.).

Eutrophication Potential (EP) for the manufacturing of the PV cell, aCPC model and the CPV system is illustrated in Fig. 12. It can be seen from the results that the total eutrophication potential for the aCPC-PV module is 9.07×10^{-4} Kg PO_4^{3-} which is mainly from the waste water and emissions to the air during the manufacturing processes of the aCPC-PV module and its additional components. To be detailed, the phosphate and the nitric oxide are two major contributors. This is related to the electricity and steam consumption whose upstream production process will release an amount of the phosphate and the nitric oxide. As for the aCPC-PV assembling process, Polyethylene terephthalate part (PET), Polyvinyl fluoride film (PVF), EVA, Encapsulation of the module (UV glue), aluminum frame are main contributors. While for the aCPC-PV module, besides the electricity consumption, the silver-coating is the other contributor to the EP.

4.4 Human Toxicity Potential (HTP)

HTP assessment focuses on the evaluation of the negative impact of a process on humans. In general, the potential of a certain substance is characterized according to its emission to the environment considering the chemical composition, physical properties, point source of emission and its behavior and whereabouts of the substance. It should be noted that the method for the life cycle impact assessment of the HTP is still in the development stage. In this study, characterization factors are calculated through the "Centre of Environmental Science (CML), Leiden University", and the National Institute of Public Health and Environmental Protection (RIVM), Bilthoven. The HTP is given in the reference of the substance 1, 4-Dichlorbenzol ($C_6H_4Cl_2$) and the unit is kg 1, 4- Dichlorbenzol-Equiv. (kg DCB-Eq.) [57].

In Fig. 13, the HTPs for the manufacturing of the PV cell, aCPC model and CPV systems are depicted. The HPT is mainly from the heavy metal and organic/inorganic emissions to the air and clean water. The heavy metal includes arsenic, chromium, nickel, selenium which are released by the production of the electricity, steam and materials that are used for the manufacturing of the aCPC-PV module. The emissions to the water are mainly dioxin which is from the wafer slicing, and hydrogen fluoride gas which is related to the electricity consumption. The emissions to the water are also mainly from the production of the electricity which includes selenium, vanadium (+3), thallium.

4.5 Ozone Layer Depletion Potential (ODP)

It is well-known that the Ozone can protect the earth because it can prevent the UV radiation from entering the ground. The short wave UV radiation is harmful to human health and the growth of the crops. However, anthropogenic emissions can deplete the ozone. There are two kinds of substances that have depletion effect, one is the fluorine-chlorine-hydrocarbons (CFCs) and the other kind is nitrogen oxides (NO_X). As for the calculation of the ODP of a specific substance, it is based on the reference of the CFC 11 (R11). So the ODP will be delivered by the kg R11-Eq./Wp for the aCPC-PV module.

The ODP of the aCPC-PV system is 6.47×10^{-8} kg R11-Eq./Wp (Fig. 14). And the emissions of the Halon (1301), carbon tetrachloride, and Halon (1211) are the main causes of the ozone layer depletion. It can be seen clearly that the aCPC-PV assembling process contributes the largest portion to the total ODP. This is related to the aluminum consumption which will generate a lot of Halon (1301) emission. As for the aCPC model and PV cell, the ODPs are mainly caused by the electricity consumption.

4.6 Photochemical Ozone Creation Potential (POCP)

Apart from playing a protective role in the stratosphere to prevent the UV radiation from entering the earth, the ozone at the ground level and in the troposphere (also known as the summer fog) may be harmful for the ecosystem. High concentration of the ozone is also toxic to the human. The ozone is produced by the complex chemical reactions between nitrogen oxides and hydrocarbons in the presence of the solar radiation. In Life Cycle Assessments, photochemical ozone creation potential (POCP) is referred in ethylene-equivalents (C_2H_4-Eq.).

The total POCP for the aCPC-PV module is calculated to be 5.77×10^{-4} kg C_2H_4-Eq./Wp (Fig. 15). Sulfur dioxide is the major contributor to the total POCP, which accounts for more than 50%. Its emission is related to the upstream production process of the electricity and steam that are used during the manufacture processes of the PV cell, the aCPC module and their assembling process. The upstream manufacturing processes of the materials such as the aluminum (for the production of the additional components), silver (for the reflective film coating), and PET/PVF/EVA/UV glue (for the assembling process) will also contribute to the POCP. In addition, non-methane volatile organic compounds (NMVOC) as well as the nitric oxide are also the contributors to the total POCP which are from the same manufacture process as the sulfur dioxide emission.

4.7 Comparison with the PV module with the same DC output

Above all, a detailed comparison of the environmental impacts for the aCPC-PV module with that of the PV module with the same DC output is listed in table 3. From the results, it can be seen clearly that the inventory categories that are selected to study the environmental profile (AP, GWP, EP, HTP, ODP, POCP) of the aCPC-PV module are all relatively lower than that of the PV module with the same DC output for the building south integration. So the superiorities of the aCPC-PV module, in terms of the price, EPBT and environment impacts are obvious as compared with the PV module.

5. Conclusions

This paper proposed a novel asymmetric lens-walled compound parabolic concentrator integration with PV (aCPC-PV) for BI application. The aCPC is composed of two asymmetric compound parabola curves which collects solar energy through the total internal reflection or the specular reflection. The experimental results show that the aCPC has a large acceptance angle up to 60° with high optical efficiency (with an average value of 74%). The maximum power gotten from the aCPC-PV to that gotten from the non-concentrating PV delivered a concentration ratio of 1.74X. A good agreement is observed between the experimental results (by the solar simulator) and the simulation results (by software Lighttools®)

An LCA study for the aCPC-PV in China is conducted. The LCIA method CML2001- Apr. 2013 based on the information gotten from the factories in China, databases of GaBi® software and Ecoinvent v3.01 are utilized. The most important conclusions derived from the study are: the primary energy demand of the aCPC-PV module is 12.2 MJ/Wp; the EPBTs of the aCPC-PV module are 2.82-4.74 years for the installation in five cities in China which are 0.2-0.3 years lower than that of the PV module with the same DC output. Considering the fact that the lifespan of the CPV system is 25 years or more which is much larger than the EPBT of the aCPC-PV module, it is practical and economical to install the aCPC-PV module on the buildings in China.

The environment impacts, such as AP, GWP, EP, HTP, ODP, POCP, are 9.16×10^{-3} SO_2-Eq./Wp, 1.09 kg CO_2-Eq./Wp, 9.07×10^{-4} kg Phosphate-Eq./Wp, 0.38 kg DCB-Eq./Wp, 6.47×10^{-8} kg R11-Eq./Wp, 5.77×10^{-4} kg Ethene-Eq/Wp, which are all relatively lower than that of the PV system with the same DC output. So it can be concluded that the aCPC-PV module is a promising concept as a cleaner technology for BI application in China. The advantages are obvious: It will reduce the use of the coal-fired power plants which will save a lot of energy, so it is more environmental friendly because it acts as a clean energy resource, causes less pollution and meets the energy demand during the production process, thus to protect the global environment. Therefore, it deserves a wider scope of application to cover the building energy demand.

Acknowledgment

The study was sponsored by the National Science Foundation of China (Grant Nos. 51408578, 51476159, 51611130195), Anhui Provincial Natural Science Foundation (1508085QE96). The authors would like to thank Prof. Zheng Hongfei (School of Mechanical Engineering, Beijing Institute of Technology, China) for his assistance in the software simulation. The authors would also like to express special thanks to the Fundamental Research Funds for the Central Universities.

References:

[1] IEA. Electricity information. International Energy Agency (IEA); 2010.

[2] M. Tripathy, H. Joshi, S.K. Panda. Energy payback time and life-cycle cost analysis of building integrated photovoltaic thermal system influenced by adverse effect of shadow. Applied Energy 2017; 208: 376-389.

[3] G. Nicoletti, N. Arcuri, G. Nicoletti, R. Bruno. A technical and environmental comparison between hydrogen and some fossil fuels. Energy Conversion and Management 2015; 89: 205-213.

[4] IEA. World energy outlook special report 2016: energy and air pollution. International Energy Agency (IEA), 2016.

[5] K. Li, H. Bian, C. Liu, D. Zhang, Y. Yang. Comparison of geothermal with solar and wind power generation systems. Renewable and Sustainable Energy Reviews 2015; 42: 1464-1474.

[6] BP. Statistical Review of World Energy; 2015.

[7] R. Bhandari, I. Stadler. Electrification using solar photovoltaic systems in Nepal. Applied Energy 2011; 88: 458-465.

[8] H. Hondo, K. Baba. Socio-psychological impacts of the introduction of energy technologies: Change in environmental behavior of households with photovoltaic systems. Applied Energy 2010; 87: 229-235.

[9] G.N. Tiwari, R.K. Mishra, S.C. Solanki. Photovoltaic modules and their applications: A review on thermal modelling. Applied Energy 2011; 88: 2287-2304.

[10] P. Balcombe, D. Rigby, A. Azapagic. Environmental impacts of microgeneration: Integrating solar PV, Stirling engine CHP and battery storage. Applied Energy 2015; 139: 245-259.

[11] Q. Zhi, H. Sun, Y. Li, Y. Xu, J. Su. China's solar photovoltaic policy: An analysis based on policy instruments. Applied Energy 2014; 129: 308-319.

[12] H. Sun, Q. Zhi, Y. Wang, Q. Yao, J. Su. China's solar photovoltaic industry development: The status quo, problems and approaches. Applied Energy 2014; 118: 221-230.

[13] U. Desideri, S. Proietti, F. Zepparelli, P. Sdringola, S. Bini. Life Cycle Assessment of a ground-mounted 1778kWp photovoltaic plant and comparison with traditional energy production systems, Applied Energy 2012; 97: 930-943.

[14] R.R.M.S. Muhammad-Sukki F.Solar concentrators in Malaysia: Towards the development of low cost solar photovoltaic systems. J. Teknologi 2011; 55: 53-65.

[15] R.M. Swanson. The Promise of Concentrators. Progress in Photovoltaics: Research and Applications2000; 8 (1): 893-111.

[16] K. Chong, S. Lau, T. Yew, P.C. Tan. Design and development in optics of concentrator photovoltaic system. Renewable and Sustainable Energy Reviews 2013; 19: 598-612.

[17]http://energy.globaldata.com/media-center/press releases/power and resources/global-concentrated-photovoltaic-cumulative-installations-to-achieve-more-than-1-gigawatt-capacity-by-2020-says-globaldata.

[18] S.H. Abu-Bakar, F. Muhammad-Sukki, R. Ramirez-Iniguez, T.K. Mallick, A.B. Munir, S.H. MohdYasin, R. Abdul Rahim. Rotationally asymmetrical compound parabolic concentrator for concentrating photovoltaic applications. Applied Energy 2014; 136: 363-372.

[19] S.H. Abu-Bakar, F. Muhammad-Sukki, D. Freier, R. Ramirez-Iniguez, T.K. Mallick, A.B. Munir, S.H. MohdYasin, A. Abubakar Mas Ud, N. MdYunus. Performance analysis of a novel rotationally asymmetrical compound parabolic concentrator. Applied Energy 2015; 154: 221-231.

[20] T.K.Mallick, P. Eames. Design and fabrication of low concentrating second generation PRIDE concentrator. Solar Energy Materials and Solar Cells 2007; 91: 597-608.

[21] Y. Su, G. Pei, S.B. Riffat, et al. A novel lens-walled compound parabolic concentrator for photovoltaic applications. Journal of Solar Energy Engineering 2012; 134 (2): 021010.

[22] G. Li, G. Pei,J. Ji, et al. Structure optimization and annual performance analysis of the lens-walled compound parabolic concentrator. International Journal of Green Energy 2016; 13 (9): 944-950.

[23] G. Li, G. Pei, Y. Su, J. Ji, S.B. Riffat. Experiment and simulation study on the flux distribution of lens-walled compound parabolic concentrator compared with mirror compound parabolic concentrator. Energy 2013; 58: 398-403.

[24] G. Li, G. Pei, Y. Su, Y. Wang, J. Ji. Design and investigation of a novel lens-walled compound parabolic concentrator with air gap. Applied Energy 2014; 125: 21-27.

[25] G. Li, G. Pei, J. Ji, M. Yang, Y. Su, N. Xu. Numerical and experimental study on a PV/T system with static miniature solar concentrator. Solar Energy 2015; 120: 565-574.

[26] G. Li, G. Pei, J. Ji, Y. Su, Outdoor overall performance of a novel air-gap-lens-walled compound parabolic concentrator (ALCPC) incorporated with photovoltaic/thermal system. Applied Energy 2015; 144: 214-223.

[27] G. Li, G. Pei, M. Yang, J. Ji, Y. Su. Optical evaluation of a novel static incorporated compound parabolic concentrator with photovoltaic/thermal system and preliminary experiment. Energy Conversion and Management 2014; 85: 204-211.

[28] G.K. Singh. Solar power generation by PV (photovoltaic) technology: A review. Energy 2013; 53: 1-13.

[29] A.F. Abd Rashid, S. Yusoff. A review of life cycle assessment method for building industry. Renewable and Sustainable Energy Reviews 2015; 45: 244-248.

[30] J. Fava, S. Baer, J. Cooper. Increasing Demands for Life Cycle Assessments in North America. Journal of Industrial Ecology 2009; 13: 491-494.

[31] O. Ortiz, F. Castells, G. Sonnemann, Sustainability in the construction industry: A review of recent developments based on LCA. Construction and Building Materials 2009; 23: 28-39.

[32] A. Sagani, J. Mihelis, V. Dedoussis. Techno-economic analysis and life-cycle environmental impacts of small-scale building-integrated PV systems in Greece. Energy and Buildings 2017; 139: 277-290.

[33] Z. Yu, W. Ma, K. Xie, G. Lv, Z. Chen, J. Wu, J. Yu. Life cycle assessment of grid-connected power generation from metallurgical route multi-crystalline silicon photovoltaic system in China. Applied Energy 2017; 185: 68-81.

[34] H. Kim, K. Cha, V.M. Fthenakis, P. Sinha, T.Hur. Life cycle assessment of cadmium telluride photovoltaic (CdTe PV) systems. Solar Energy 2014; 103: 78-88.

[35] J. Hong, W. Chen, C. Qi, L. Ye, C. Xu. Life cycle assessment of multicrystalline silicon photovoltaic cell production in China. Solar Energy 2016;133: 283-293.

[36] P. Jayathissa, M. Jansen, N. Heeren, Z. Nagy, A. Schlueter. Life cycle assessment of dynamic building integrated photovoltaics. Solar Energy Materials and Solar Cells 2016; 156: 75-82.

[37] V. Kabakian, M.C. McManus, H. Harajli.Attributional life cycle assessment of mounted 1.8kWp monocrystalline photovoltaic system with batteries and comparison with fossil energy production system. Applied Energy 2015; 154: 428-437.

[38] L. Lu, H.X. Yang. Environmental payback time analysis of a roof-mounted building-integrated photovoltaic (BIPV) system in Hong Kong. Applied Energy 2010; 87: 3625-3631.

[39] G. Hou, H. Sun, Z. Jiang, Z. Pan, Y. Wang, X. Zhang, Y. Zhao, Q. Yao. Life cycle assessment of grid-connected photovoltaic power generation from crystalline silicon solar modules in China. Applied Energy 2016; 164: 882-890.

[40] C. Lamnatou, H. Baig, D. Chemisana, T.K. Mallick. Life cycle energy analysis and embodied carbon of a linear dielectric-based concentrating photovoltaic appropriate for building-integrated applications. Energy and Buildings 2015; 107: 366-375.

[41] C. Lamnatou, H. Baig, D. Chemisana, T.K. Mallick. Environmental assessment of a building-integrated linear dielectric-based concentrating photovoltaic according to multiple life-cycle indicators. Journal of Cleaner Production 2016;

131: 773-784.

[42] C. Lamnatou, H. Baig, D. Chemisana, T.K. Mallick, Dielectric-based 3D building-integrated concentrating photovoltaic modules: An environmental life-cycle assessment. Energy and Buildings 2017; 138: 514-525.

[43] K. Menoufi, D. Chemisana, J.I. Rosell. Life Cycle Assessment of a Building Integrated Concentrated Photovoltaic scheme. Applied Energy 2013; 111: 505-514.

[44] V.M. Fthenakis, H.C. Kim. Life cycle assessment of high-concentration photovoltaic systems. Progress in Photovoltaics: Research and Applications 2013; 21: 379-388.

[45] G. Peharz, F. Dimroth. Energy payback time of the high-concentration PV system FLATCON®. Progress in Photovoltaics: Research and Applications 2005; 13: 627-634.

[46] A. Nishimura, Y. Hayashi, K. Tanaka, M. Hirota, S. Kato, M. Ito, K. Araki, E.J. Hu. Life cycle assessment and evaluation of energy payback time on high-concentration photovoltaic power generation system. Applied Energy 2010; 87: 2797-2807.

[47] Y. Fu, X. Liu, Z. Yuan. Life-cycle assessment of multi-crystalline photovoltaic (PV) systems in China. Journal of Cleaner Production 2015; 86: 180-190.

[48] R.Dones, R. Frischknecht. Life-cycle assessment of photovoltaic systems:results of Swiss studies on energy chains. Progress in Photovoltaics: Research and Application 1998;6: 117-125.

[49] T.K. Mallick, P.C. Eames, T.J. Hyde, B. Norton. The design and experimental characterisation of an asymmetric compound parabolic photovoltaic concentrator for building facade integration in the UK. Solar Energy 2004; 77: 319-327.

[50] Y. Su, S.B. Riffat, G. Pei. Comparative study on annual solar energy collection of a novel lens-walled compound parabolic concentrator (lens-walled CPC), Sustainable Cities and Society 2012; 4: 35-40.

[51] A. Rabl, J. O'Gallagher, R. Winston. Design and test of non-evacuated solar collectors with compound parabolic concentrators. Solar Energy 1980; 25: 335-351.

[52] ISO 14040:2006, Environmental Management – Life Cycle Assessment – Principles and Framework.

[53] ISO 14044:2006, Environmental Management – Life Cycle Assessment – Requirements and Guidelines.

[54] Methodology principles: Guinée, J.B.; Gorrée, M.; Heijungs, R.; Huppes, G.; Kleijn, R.; Koning, A. de; Oers, L. van; Wegener Sleeswijk, A.; Suh, S.; Udo de Haes, H.A.; Bruijn, H. de; Duin, R. van; Huijbregts, M.A.J. Handbook on life cycle assessment. Operational guide to the ISO standards. I: LCA in perspective. IIa: Guide. IIb: Operational annex. III: Scientific background. Kluwer Academic Publishers, ISBN 1-4020-0228-9, Dordrecht, 2002, 692 pp.

[55] Characterisation factors: cml.leiden.edu/software/data-cmlia.html.

[56] Hay, J.E., Davies, J.A. Calculation of the solar radiation incident on an inclined surface. Proceedings of the First Canadian Solar Radiation Data Workshop 1980;

59-72.

[57] GUINÉE ET AL. 2002. Handbook on Life Cycle Assessment: An operational Guide to the ISO Standards; Dordrecht: Kluvver Academic Publsihers, 2002.

[58] M. Raugei, S. Bargigli, S. Ulgiati. Life cycle assessment and energy pay-back time of advanced photovoltaic modules: CdTe and CIS compared to poly-Si. Energy 2007; 32: 1310-1318.

Figure captions

Fig. 1 The structure of the aCPC.

Fig.2 Configuration of the aCPC-PV module.

Fig.3 The prototype of the aCPC structure and the experiment setup.

Fig.4 The optical efficiency of the aCPC at different incidence angles.

Fig.5 Life cycle of the aCPC-PV module.

Fig.6 Primary energy demand for the aCPC-PV module (for 1 kWp) aCPC.

Fig.7 Schematic of the incidence angle for the aCPC.

Fig.8aCPC-PV electrical DC output (kWh/kWp) per month for five different cities in China: (a) with the experimental optical efficiency and (b) with the simulation optical efficiency.

Fig.9 Energy payback time of the aCPC-PV module and the normal PV module.

Fig.10 Acidification Potential (AP) for the aCPC-PV module.

Fig.11 Global Warming Potential (GWP 100 years) for the aCPC-PV module.

Fig.12 Eutrophication Potential (EP) for the aCPC-PV module.

Fig.13 Human Toxicity Potential (HTP) for the aCPC-PV module.

Fig.14 Ozone Layer Depletion Potential (ODP) for the aCPC-PV module.

Fig.15 Photochemical Ozone Creation Potential (POCP) for the aCPC-PV module.

Table captions

Table 1 Life cycle inventory (LCI): materials/characteristic of the studied aCPC-PV module.

Table 2 Annual irradiance on the building south wall (per m^2), electricity production of the studied aCPC-PV module (for 1kWp).

Table 3 Comparison of the environmental impacts of the aCPC-PV module with that of the PV module with the same DC output.

Nomenclature

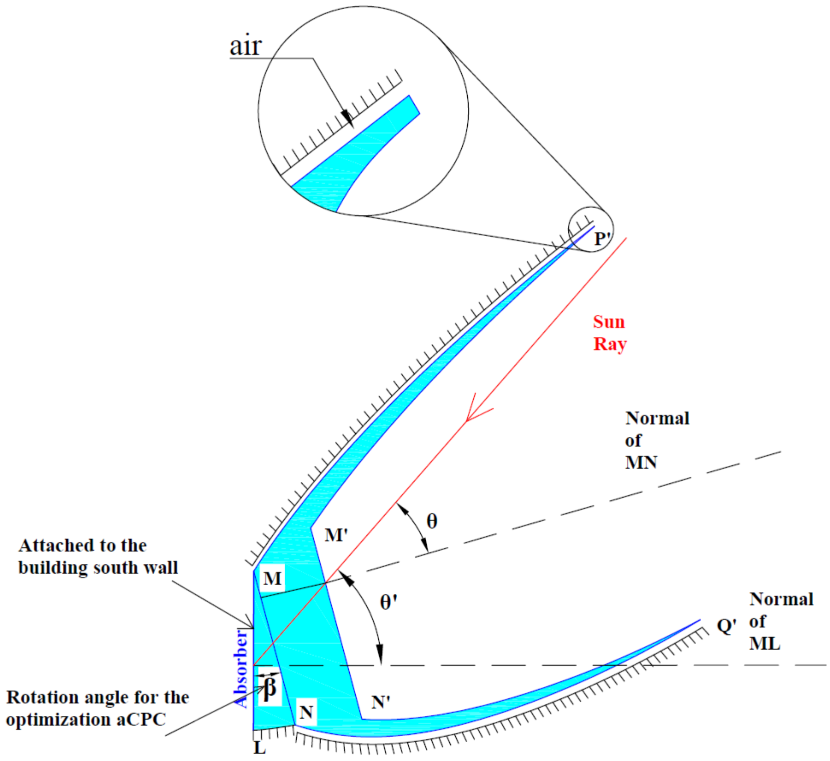

Fig. 1 The structure of the aCPC.

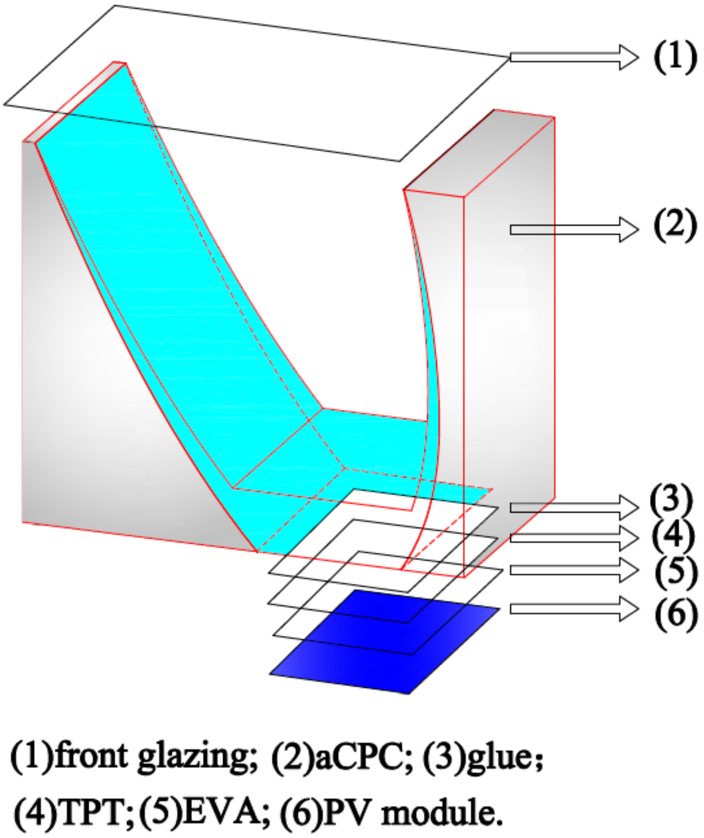

Fig.2 Configuration of the aCPC-PV module.

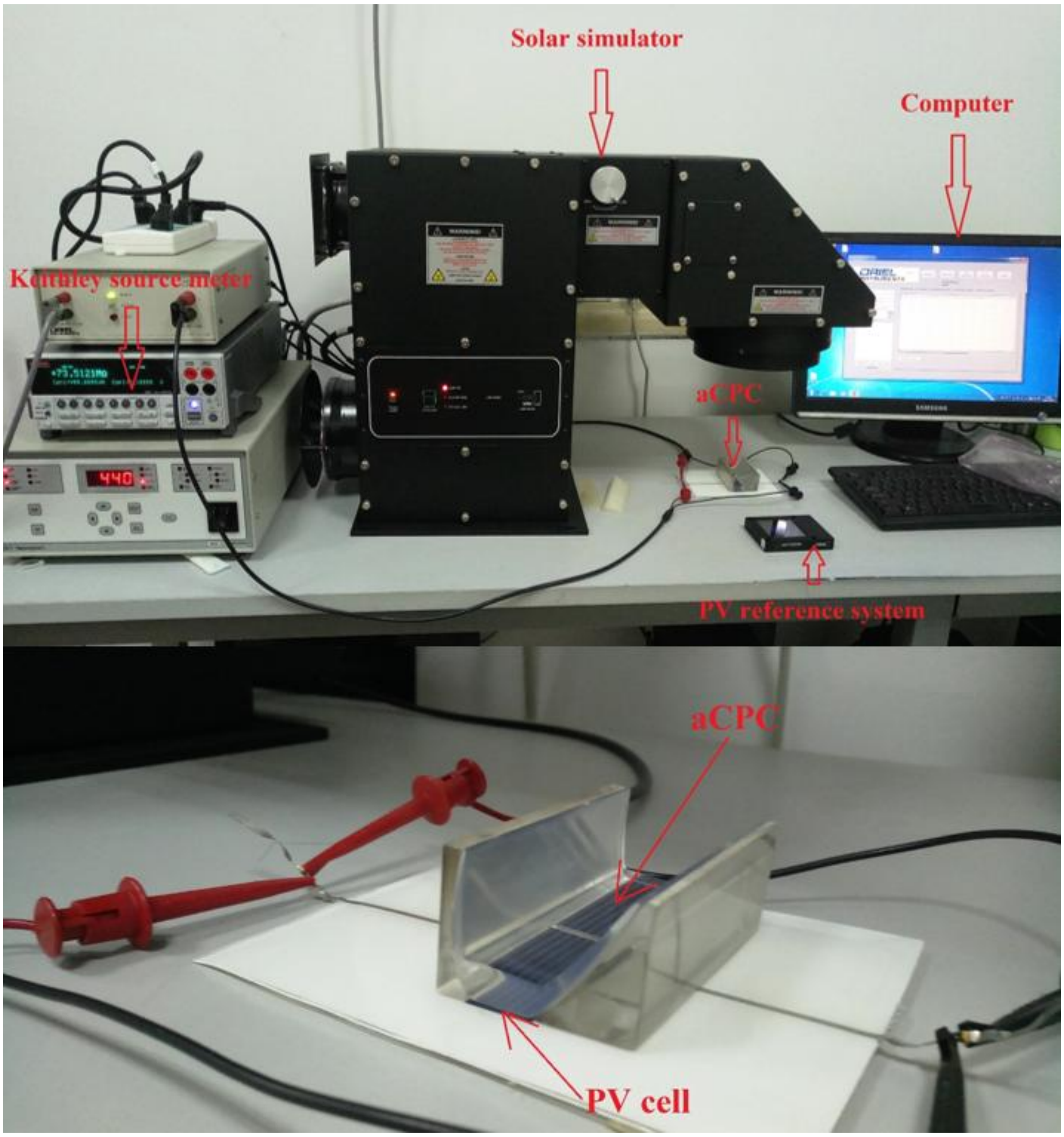

Fig. 3 The prototype of the aCPC structure and the experiment setup.

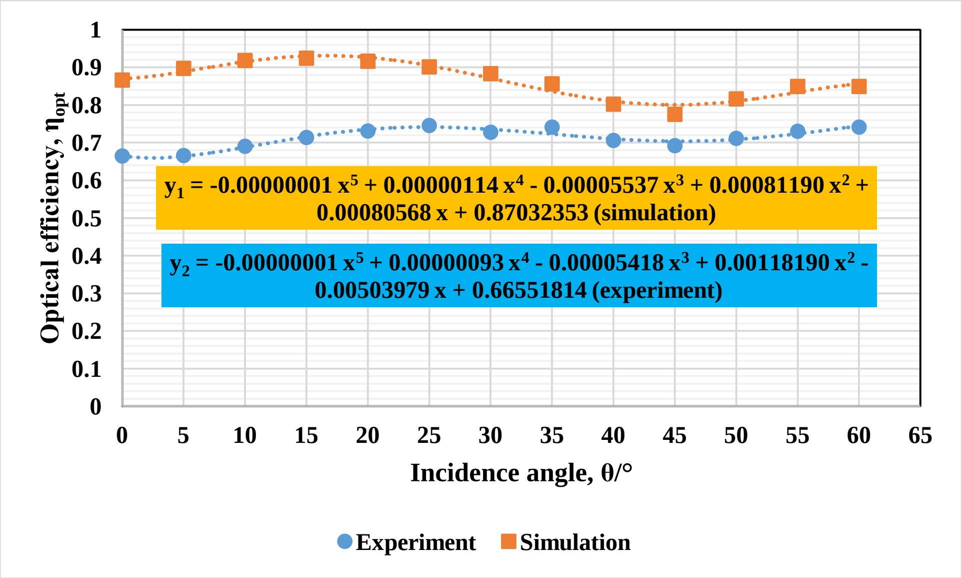

Fig. 4 The optical efficiency of the aCPC at different incidence angles.

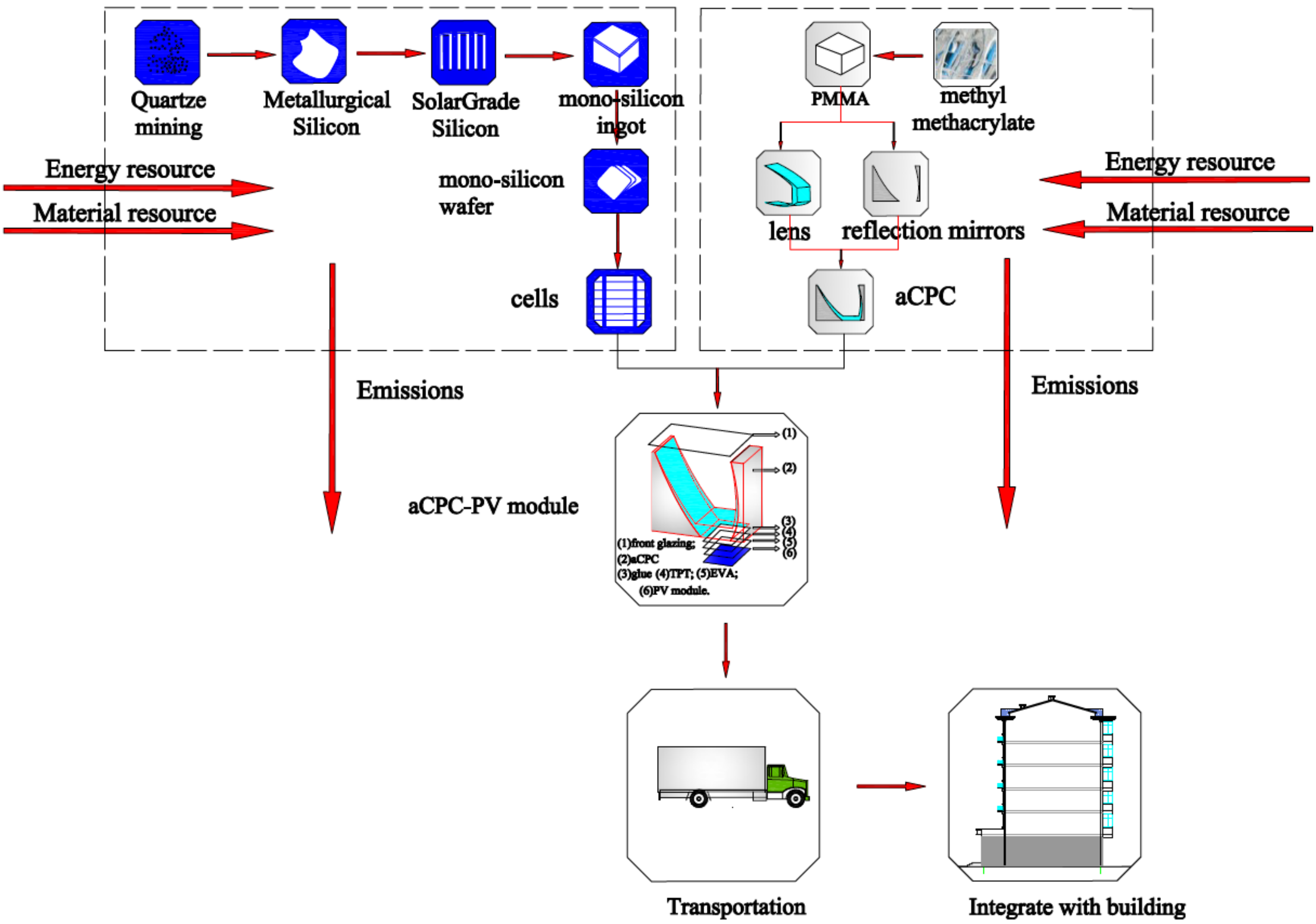

Fig. 5 Life cycle of the aCPC-PV module.

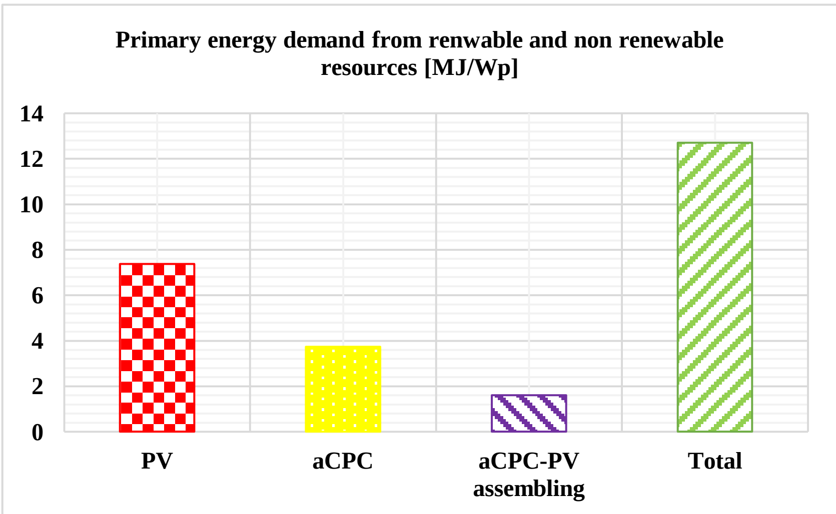

Fig.6 Primary energy demand for the aCPC-PV module (for 1 kWp).

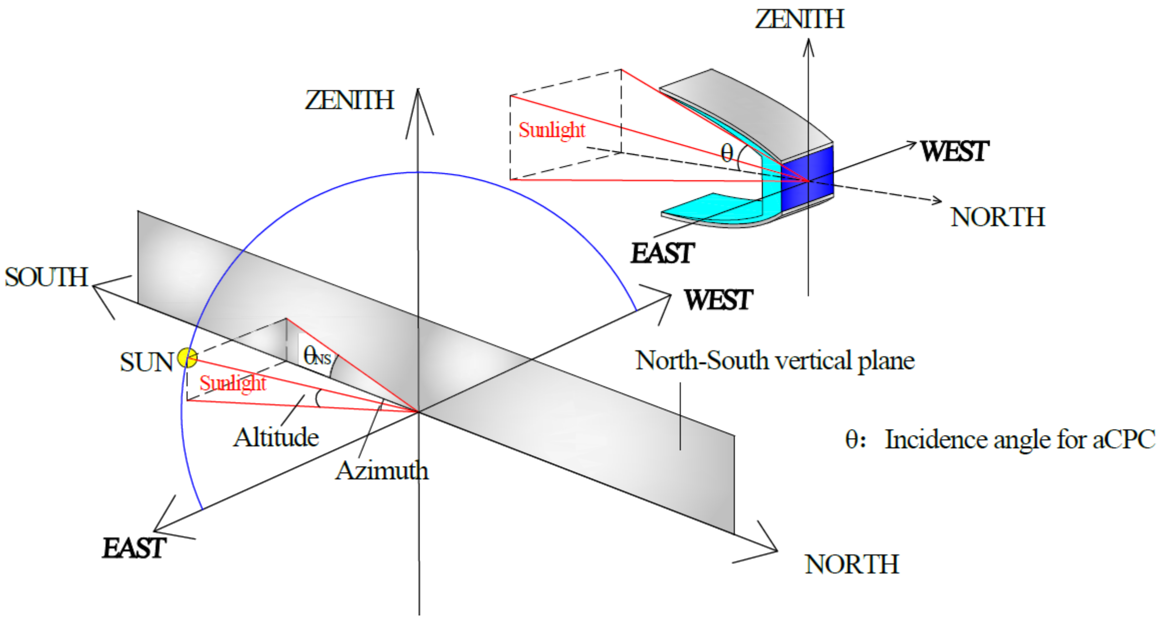

Fig. 7 Schematic of the incidence angle for the aCPC.

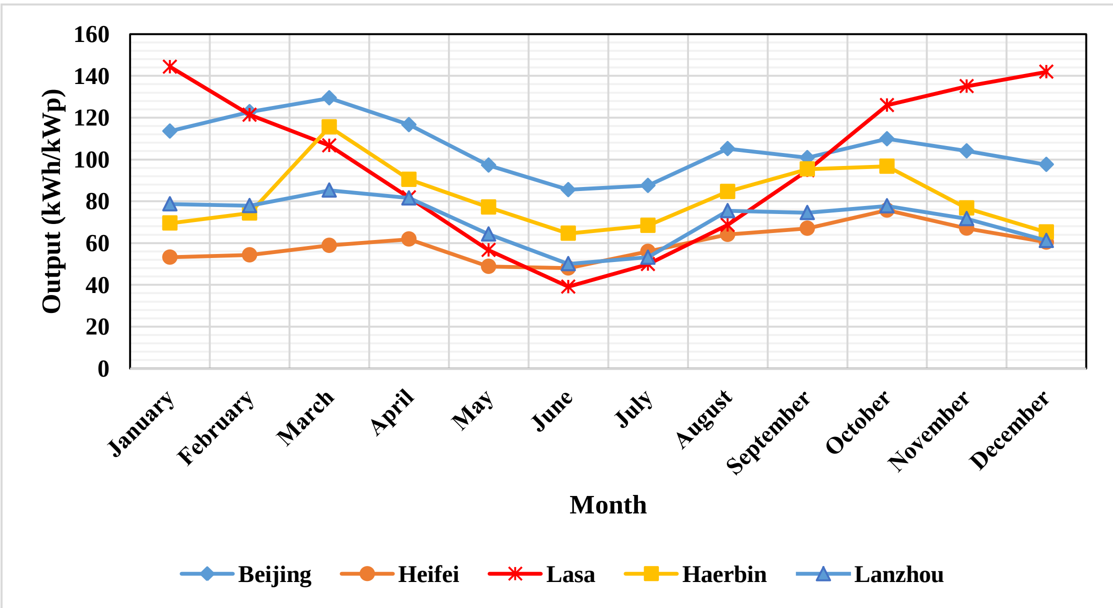

(a)

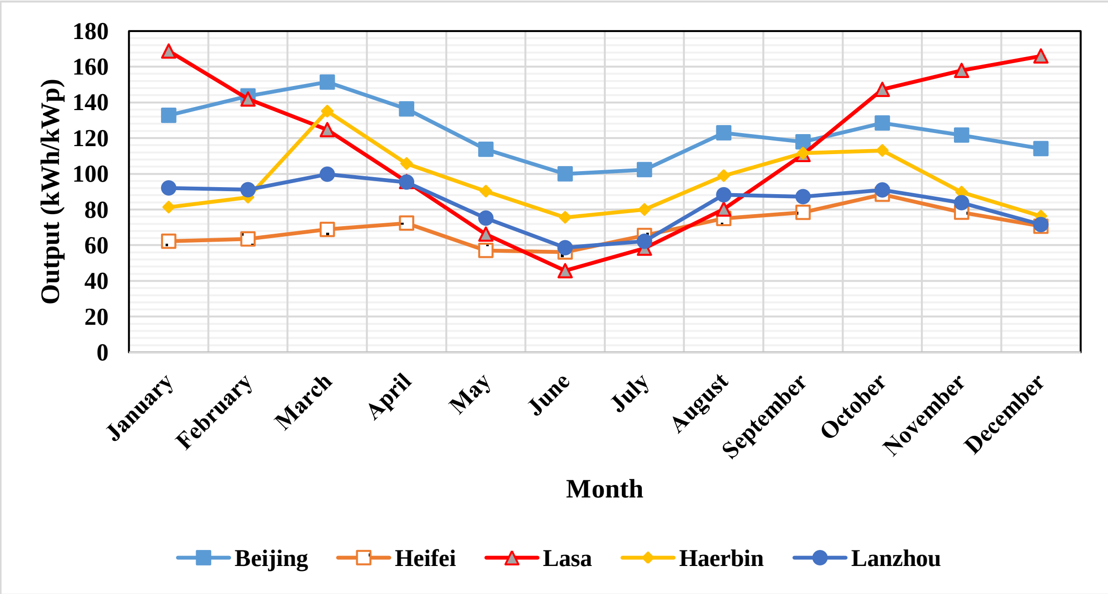

(b)

Fig. 8aCPC-PV electrical DC output (kWh/kWp) per month for five different cities in China: (a) with the experimental optical efficiency and (b) with the simulation optical efficiency.

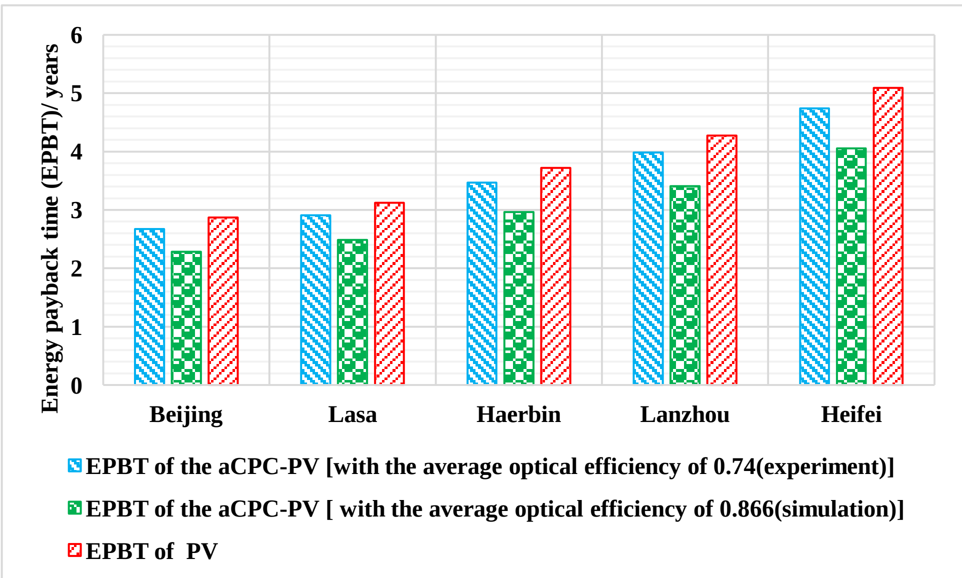

Fig. 9 Energy payback time of the aCPC-PV module and the normal PV module.

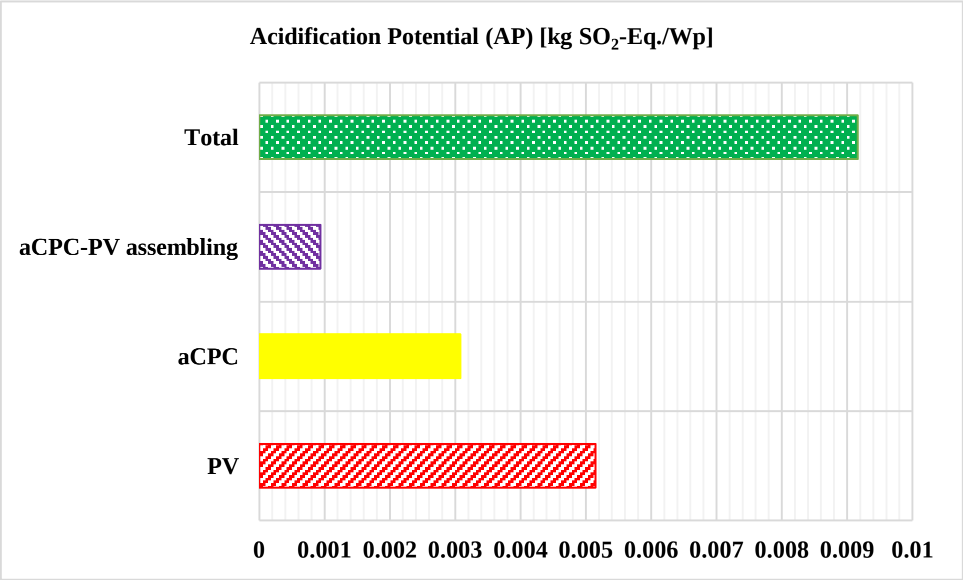

Fig. 10 Acidification Potential (AP) for the aCPC-PV module.

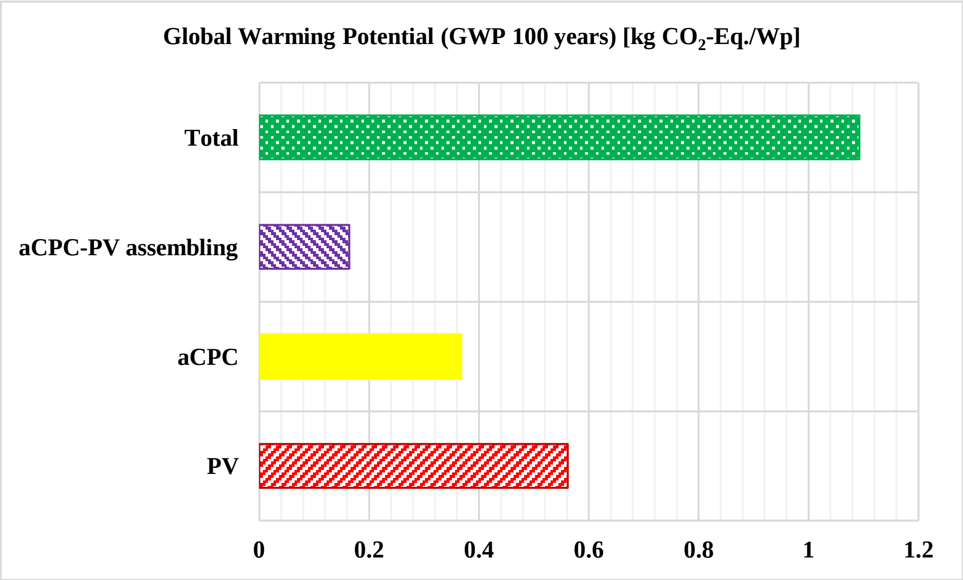

Fig.11 Global Warming Potential (GWP 100 years) for the aCPC-PV module.

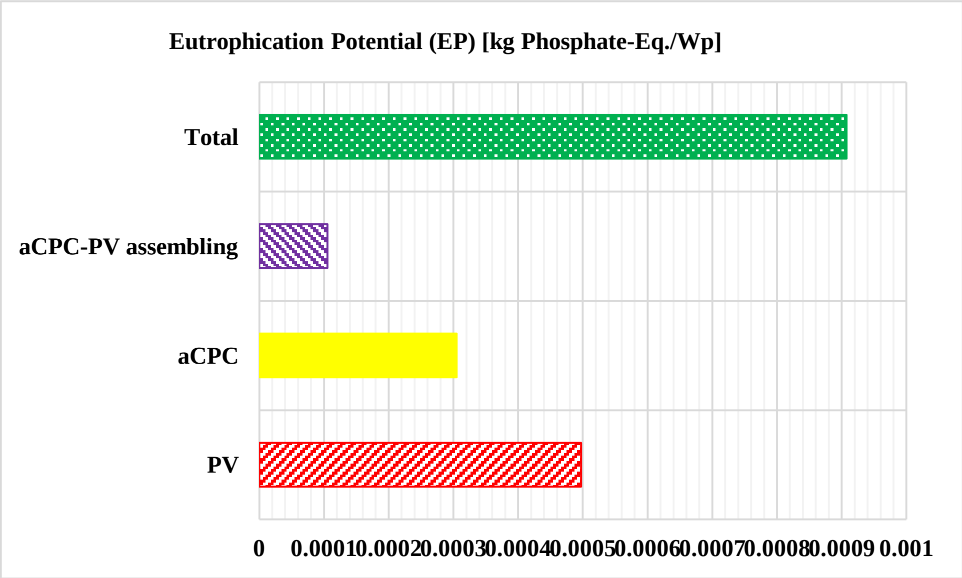

Fig. 12 Eutrophication Potential (EP) for the aCPC-PV module.

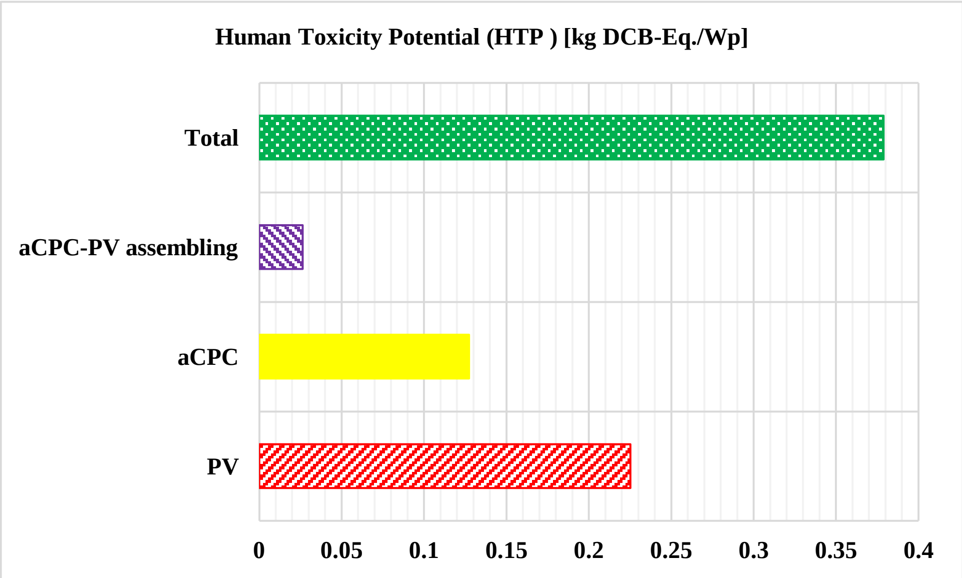

Fig. 13 Human Toxicity Potential (HTP) for the aCPC-PV module

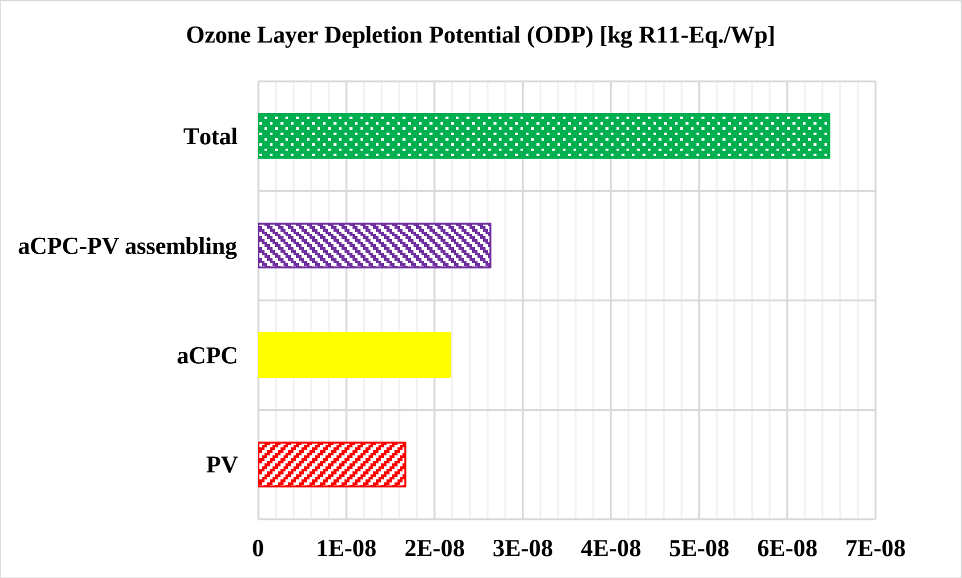

Fig. 14 Ozone Layer Depletion Potential (ODP) for the aCPC-PV module.

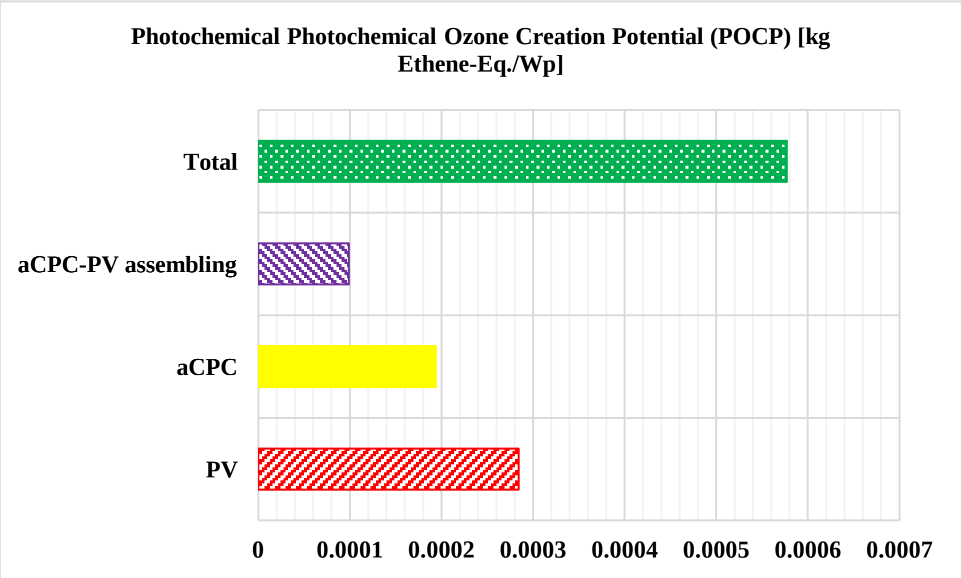

Fig. 15 Photochemical Ozone Creation Potential (POCP) for the aCPC-PV module

Table 1. Life cycle inventory (LCI): materials/characteristic of the studied aCPC-PV module

Materials/Characteristics for 1kWp module	Description/(-/kWp)
aCPC/ kg	74.9
PV cells/ m^2	3.32
Average optical efficiency of the aCPC	74%
Efficiency of the cells	16%
Front glass of the module/ kg	43.4
Reflective film (silver-coated acrylic)/ kg	0.05
Polyethylene terephthalate part (PET)/ kg	1.97
Polyvinyl fluoride film (PVF) / kg	1.97
EVA/ kg	2.721
Encapsulation of the module (UV glue)/ kg	1.612
Aluminum frame/ kg	5.89 [58]
Cables and contact boxes (copper)/ kg	0.124 [58]
Cables and contact boxes (plastics)/ kg	0.124 [58]

The impact is calculated per kWp of aCPC-PV module output.

Table 2 Annual irradiance on the building south wall (per m^2), electricity production of the studied aCPC-PV module (for 1kWp).

	Beijing	Lhasa	Lanzhou	Harbin	Hefei
Annual irradiance: kWh/m^2 year	1280.37	1176.27	987.34	859.02	721.56
Electricity production: kWh per year	1269.60	1165.69	851.30	978.46	715.07
Electricity production: kWh for 20 years lifespan	21100.22	19373.26	14148.18	16261.67	11884.17
Electricity production: kWh for 30 years lifespan	28852.62	26491.16	26491.16	22236.35	16250.51

Table 3 Comparison of the environmental impacts of the aCPC-PV module with that of the PV module with the same DC output.

LCIA category	aCPC-PV module (per Wp)	PV module (Wp)
AP/kg SO_2-Eq.	9.16×10^{-3}	1.04×10^{-2} [47]
GWP (100 years)/kg CO_2-Eq.	1.09	1.24 [47]
EP/kg Phosphate-Eq.	9.07×10^{-4}	1.03×10^{-3} [47]
HTP/kg DCB-Eq.	0.38	0.43[47]
ODP/kg R11-Eq.	6.47×10^{-8}	7.35×10^{-8} [47]
POCP/kg Ethene-Eq.	5.77×10^{-4}	6.55×10^{-4} [47]

Nomenclature

aCPC	Asymmetric lens-walled compound parabolic concentrator	ODP	Ozone Layer Depletion Potential
A	the area of the front aperture, m^2	PMMA	polymethyl methacrylate
AP	Acidification Potential	POCP	Photochemical Ozone Creation Potential
A_i	Anisotropy index	R_b	View factor for beam radiation
BOS	balance of system	Greek symbols	
C	geometric concentration ratio	α	solar altitude angle
CML	CML method	β	rotation angle
DC	direct current	θ	incidence angle for the aCPC
EP	Eutrophication potential	θ'	incidence angle for the optimization aCPC
EPBT	energy payback time, years	θ_T	incidence angle of the solar rays on the decline surface
E_{agen}	annual electricity generation	θ_Z	Zenith angle
GWP	Global Warming Potential	φ	Latitude angle
G_{dir}	the total direct solar irradiance on the building south wall, Wm^{-2}	δ	declination angle of the sun

G_{diff}	the diffuse solar irradiance on the building south wall, Wm^{-2};	γ	azimuth angle of the declination surface
HTP	Human Toxicity Potential	γ_s	solar azimuth angle
I	total solar radiation on the horizontal surface, Wm^{-2}	λ	declination angle
$I_{southwall}$	solar radiation on the building south wall, Wm^{-2}	ρ	the reflectivity of the ground;
I_b	direct solar radiation on the horizontal surface, Wm^{-2}	ω	Hour angle
I_d	diffuse solar radiation on the horizontal surface, Wm^{-2}	η_{opt}	optical efficiency of the aCPCA
LCA	life-cycle assessment	$\eta_{opt,diff}$	the optical efficiency for the collection of the diffuse solar radiation
LCIA	life-cycle impact assessment	$\eta_{efficiency}$	the electrical efficiency of the PV cell
MMA	Methl Methacrylate		